Photodissociation of Nitrous Oxide by Slice Ion Imaging: The Stagnation Pressure Dependence

Nu Ri Cheong, Hye Sun Park, Sang Hwan Nam, Seung Keun Shin, Soo Gyeong Cho,[†] Hai Whang Lee,[‡] Jae Kyu Song,[*] and Seung Min Park[*]

Department of Chemistry, Kyunghee University, Seoul 130-701, Korea
[*]E-mail: jaeksong@khu.ac.kr (JKS); smpark@khu.ac.kr (SMP)
[†]Agency for Defense Development, P. O. Box 35-5, Yuseong, Daejeon 305-600, Korea
[‡]Department of Chemistry, Inha University, Incheon 402-751, Korea
Received June 29, 2009, Accepted September 17, 2009

Photodissociation of nitrous oxide near 203 nm has been studied by a combination of high resolution slice ion imaging technique and (2+1) resonance-enhanced multiphoton ionization (REMPI) spectroscopy of $N_2(X^1\Sigma_g^+)$ *via* the $(a''^1\Sigma_g^+)$ state. We have measured the recoil velocity and angular distributions of N_2 fragments by ion images of the state-resolved photofragments. The N_2 fragments were highly rotationally excited and the NN-O bond dissociation energy was determined to be 3.635 eV. Also, we investigated the photofragment images from the photodissociation of N_2O clusters with various stagnation pressures.

Key Words: Slice ion imaging, Photodissociation, Cluster

Introduction

Photofragment translational spectroscopic studies have been widely employed to abstract information regarding the angular and kinetic energy distributions of photofragments as well as their quantum states caused by photodissociation for relatively simple molecules. In late 1980s, Chandler and Houston pioneered this research area, starting from their 2-dimensional ion imaging study on photodissociation of CH_3I.[1] While a time-of-flight (TOF) method help understand the kinetic energy release from temporal analyses, the ion imaging method turns out to be exceptionally powerful to verify angular distributions as well as kinetic information of the products. Eppink and Parker[2] improved spatial resolutions of ion and electron images replacing the grids with simple focusing electrodes, which can remove blurring of images effectively.

Later, ion imaging technique has met a new aspect *via* suggestion of '*slice imaging*' which is characterized by a delayed pulsed extraction introduced by Kitsopoulos and coworkers.[3] In recent years, diverse slice ion imaging techniques have been developed to overcome the drawbacks stemming from reconstruction of the 2-dimensional image to a 3-dimensional one *via* inverse Abel transformation. By slice imaging methods, images with higher resolutions are available even without any indirect analytic tools. Besides, it is easy to understand temporal structures of fragment ion spheres in crossed molecular beam experiments.[4]

Among many molecules, N_2O has been one of the most attractive target molecules for photodissociation imaging studies due to the rich information available from spectroscopic and dynamical studies of its photodissociation.[5-12] Neyer *et al*.[8] have reported the photofragment images of N_2 with J-dependent anisotropy and Suzuki and coworkers[11,12] have shown high resolution images of N_2 and O fragments and determined the contribution of two excited states of N_2O molecule in photoabsorption.

Recently, photodissociation of weakly bound van der Waals clusters has been studied employing the ion imaging technique.[13] Here, we introduce our new slice ion imaging apparatus on the basis of time-sliced ion velocity mapping technique using ion optics with many electrodes assembly suggested by Kitsopoulos[4] and attempt to verify the effects of the stagnation pressure on the formation of N_2O clusters and their photodissociation at ultraviolet region[5-12] Previously, infrared spectroscopic studies of N_2O clusters have been performed to examine their predissociation processes, together with structural information.[14-20]

Experimental

Figure 1 shows a schematic representation of the experimental setup for slice ion imaging. The chamber consists of two parts; a source chamber and an ion flight chamber. They were installed in vertical direction to minimize any possible distortion and tilting of ion optics due to the gravitational force. The ion optics consists of total 28 electrodes with circular holes, whose outer diameter and thickness are 140 mm and 1.0 mm, respectively. Voltages supplied to the first, the second, and the third electrode along the ion flight pathway are designated as V_R, V_E and V_L, the inner diameters (i.d.) of the center holes being 2 mm, 40 mm, and 40 mm, respectively. The other electrodes, from the fourth to the last, have same dimensions (i.d. = 60 mm). The spacing between the two electrodes for the first three electrodes is 2.54 cm. The other electrodes are 1.59 cm apart with each other, each being coupled with 1 MΩ resistance to evenly divide the voltage supplied to V_L.

The ions generated by dissociation and subsequent ionization fly through the ion optics holes. The first and the second fields felt by the ions are nearly equal (~47 V/cm) and the ion sphere moves slowly toward the third strong field (~106 V/cm). V_E determines a length of the ion sphere and V_L controls a

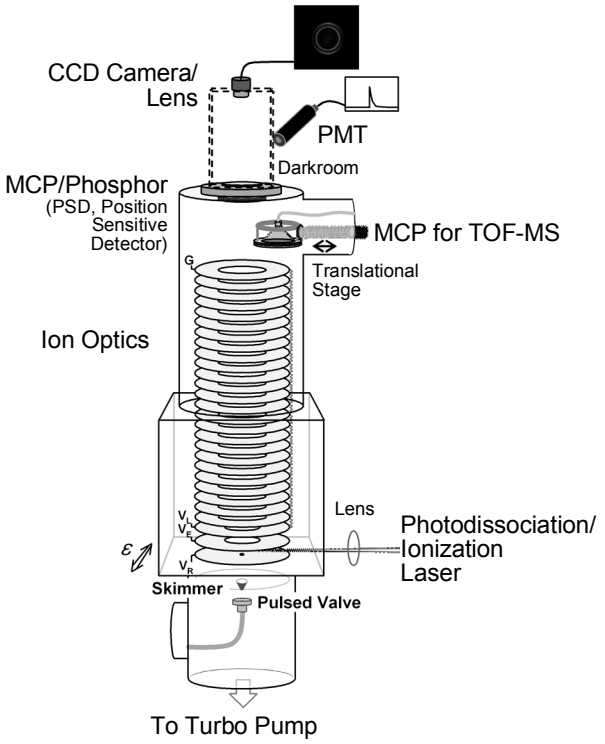

Figure 1. Schematic representation of the velocity map slice ion imaging apparatus. Two different detectors, one for imaging and the other for time-of-flight mass spectroscopy are selected by a translational stage.

focusing of the ion trajectory. Images with optimum resolution are to be obtained by adjusting these two voltages. For detecting ions, we can choose either an ordinary MCP (micro channel plate) detector for time of flight (TOF) mass spectroscopy or an imaging MCP/phosphor detector (Photonics, P20, diameter = 40 mm). The ordinary MCP detector is mounted on a translational stage so that it can be pulled away when images are obtained. The flight length for the ions as measured from the ionization spot to the front surface of the imaging MCP detector is 65 cm. The light emission from the phosphor screen, generated as the ions impinge on the imaging MCP detector, is accumulated by a charge coupled device (CCD) camera (Sony, XC-HR70) which is mounted in a black box to reduce interference from stray lights.

A key point for slice imaging technique is to take the central ion spots of Newton sphere selectively, which have only v_x and v_y components along z-axis flight pathway, produced by ionized fragments. With many electrodes arrangement, a gradual increment of the electric field can lengthen the z-axis length of the sphere effectively without any distortion. This is the opposite configuration compared with the TOF setup. We set the voltages $V_R/V_E = \sim 0.98$, $V_R/V_L = \sim 0.95$ for imaging and $V_R/V_E = \sim 0.73$, V_L = ground for TOF analysis, respectively.

Although a shorter mass gate width of the imaging detector can give an image with a higher resolution, it needs to be adjusted without sacrificing too much ion signal intensity. The gate width is set at 70 ns, but the effective gating time is 20 ~ 30 ns, considering the rise and decay time of the high voltage pulser. To avoid a blurred image, the minimization of the central spot size is a prerequisite, which is to be obtained by supplying higher MCP and lower phosphor voltages. For data acquisition and analysis of ion images, we adopt a real time ion counting method, using the programs developed by Suits and co-workers.[20] The velocity calibration is performed by analysis of O^+ image from 4-photon dissociation/ionization of O_2 molecules at 224.999 nm.[2,4,21] The velocity resolution is 0.89% ($\delta v/v$) at a kinetic energy release (KER) of ~1.6 eV.

We chose the photodissociation study of N_2O molecules at 202 - 204 nm regions to confirm the accuracy of our experimental results from our imaging system. Several researchers have performed the photodissociation of N_2O[6,8,11,12] to N_2 and O fragments via one-photon absorption, where N_2 fragments are detected by (2+1) photon ionization process. A mixed gas of 20% N_2O in He carrier gas is supersonically expanded using a pulsed valve. The laser beam for dissociation of N_2O molecules is generated by doubling and mixing of visible output (606 - 612 nm) produced by a dye laser (Lumonics) pumped by a Nd:YAG laser (Spectra Physics, GCR150-10) using a beta barium borate (BBO) crystal. The laser beam is properly focused using a lens (f = 250 mm) to achieve the 4-photon process after separating from visible and doubled beams using a 4-Pellin-Broca prism assembly. Care has been taken to avoid a space charge effect by maintaining the laser power as low as possible. The stagnation pressure was varied from 2.5 to 25 psi to observe clustering effects of N_2O molecules. Also, (2+1) REMPI spectra of N_2 are obtained at different stagnation pressures.

Results and Discussion

Figure 2(a) shows the slice ion image of N_2 fragment prod uced by one-photon dissociation of N_2O, which produces $O(^1D)$ by the reaction of $N_2O \rightarrow N_2(X^1\Sigma_g^+) + O(^1D)$, followed by (2+1) resonance-enhanced multiphoton ionization (REMPI) *via* the $(a''^1\Sigma^+)$ state at ~203 nm ($v = 0$, $J = 66$). This is the raw image, accumulated by a center of mass calculation of each ion spot using a real time ion counting program.[20] Figure 2(b) and 2(c) show translational energy and angular distributions of the N_2 fragment in a single quantum state of $v = 0$, $J = 66$. The image indicates a symmetrically sharp ring from (0,0,0) state of N_2O and also gives a higher energy ring from a vibrationally excited molecule at (0,1,0) state. A terminal splitting of the ring from the (0,0,0) level is caused by the energy taken away from the photoelectron when the nitrogen is ionized.[12] The calculated anisotropy parameter value (β) obtained from the angular distribution was 0.83.

We observed N_2 images at several rotational quantum states and determined NN-O bond dissociation energy (D_0) from a state-selected N_2 image at $v = 0$ and $J = 74$. D_0 is obtained from the equation, $D_0 = h\nu + E_{int} - \{E_{vib}(v) + B_v J(J+1) - D_v J^2(J+1)^2\} - E_{trans}(v,J)$. The rotational and centrifugal constants for calculations are used from the previous work (ν_{00}=98840.10, B_0'= 1.91429 and D_0'=6.133 × 10^{-6} cm^{-1}).[11] The estimated bond dissociation energy is 3.635 eV which is in good agreement with the reference value (3.630 eV) at the same J state.[11]

Figure 3(a), (b), and (c) show the slice ion images of N_2 frag-

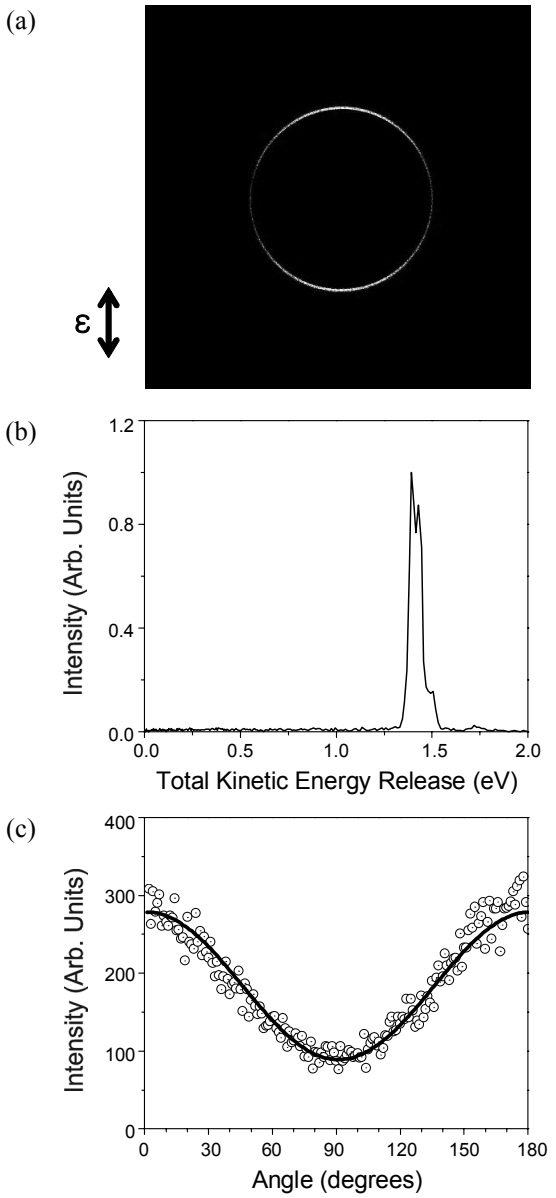

Figure 2. (a) Raw ion image of $N_2(^1\Sigma_g^+)$ fragment from N_2O dissociation. (b) Total translational energy distribution, and (c) angular distribution taken from the image in a quantum state of $v = 0, J = 66$. The calculated anisotropy (β) is 0.83. The stagnation pressure is 2.5 psi.

ment at different stagnation pressures. A concentrated cloud is clearly observed at the central part of N_2 image at high pressure as shown in Fig. 3(a) and 3(b), while it disappears at 12 psi. Figure 3(d) shows translational energy distributions of the N_2 fragments at different pressures. The translational distribution consists of two components; one is the fast component with kinetic energy of 0.52 eV and the other is the slow one with 0.008 eV, which represents the cloud image at the center.

Figure 4(a) and 4(b) show the (2+1) REMPI spectra of nascent $N_2(X^1\Sigma_g^+)$ produced by one-color photodissociation of N_2O in a supersonic molecular beam. The N_2 fragments are highly rotationally excited, and the overall spectral features are in excellent agreement with those reported by Hanisco and

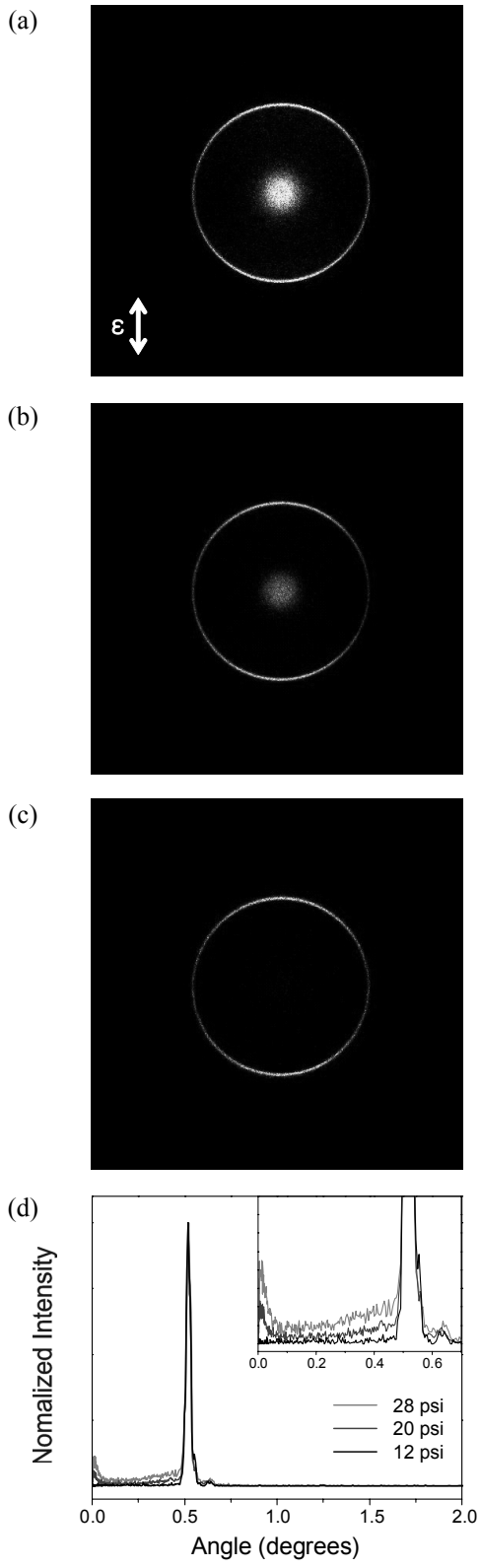

Figure 3. Raw ion images of N_2 fragment with various stagnation pressures at a same quantum state, $v = 0, J = 66$; (a) 28, (b) 20, and (c) 12 psi, (d) their N_2 translational energy distributions, normalized at intensity of (0,0,0) level.

Kummel.[6] It is of note that the $N_2(X^1\Sigma_g^+)$ rotational state distribution for 2.5 psi pressure is considerably hotter than that

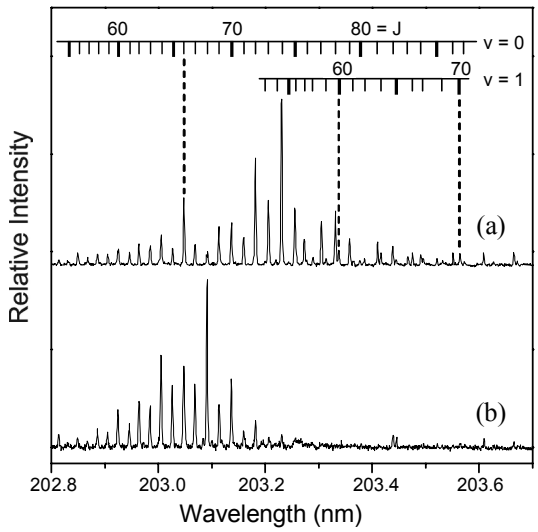

Figure 4. The (2+1) REMPI spectra of N_2 fragment from the dissociation of N_2O at different stagnation pressures; (a) 2.5 psi and (b) 25 psi. The intensity is normalized at each maximum peak. The rotational distribution is shifted to a lower rotational state at a relative high stagnation pressure.

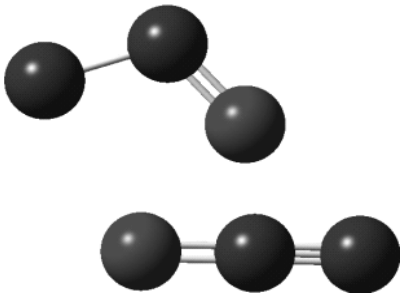

Figure 5. The optimized structure of the excited N_2O dimer.

for 25 psi pressure.

The optimized structure of the excited N_2O dimer has been calculated with the GAUSSIAN03 program package at the B3LYP/cc-pVDZ level. The most stable structure is displayed in Fig. 5.

Infrared spectroscopic studies about N_2O clusters such as dimer, trimer, and tetramer have been reported with interests of van der Waals clusters. Miller *et al*. have shown quadruple mass spectra for N_2O at various source pressures.[15,16] Their cluster-size distributions show dominant monomer with relatively weak dimer and trimer peaks even at high pressure conditions ranging from 32 to 218 psi. In this regard, our molecular beam is considered to consist mainly of monomers with small amount of dimer clusters at ~25 psi stagnation pressure. The intensity of the central cloud increases with the stagnation pressure, which is attributed to the slow N_2 fragments produced by dissociation of N_2O dimer.

At the ground electronic state, N_2O dimer gives a linear structure forming a weakly bound van der Waals complex. When N_2O dimer is electronically excited, a monomer becomes bent as it gets excited. The rotational motion of the fragment N_2 is hindered due to the formation of dimer. Also, its kinetic energy decreases since a significant portion of the kinetic energy is transferred to the neighboring molecule before the fragment N_2 molecule flies away. This explains the cloud image of N_2 at the center. However, further investigations are required to confirm the above-mentioned mechanism.

Conclusion

We constructed a slice ion imaging apparatus by using many electrodes optics which give high resolution ion images supplying gradual increasing electric field to enlarge the ion sphere. We examined the photodissociation of nitrous oxide at the wavelength range from 202 to 204 nm to confirm the experimental accuracy of our setup. The bond dissociation energy of NN-O was 3.635 eV, which is quite close to the reference value, 3.630 eV. The central cloud images became apparent with the increase of pressure, which is considered to originate from the photodissociation of N_2O clusters.

Acknowledgments. This work was supported by the National Research Foundation of Korea (No. 2009-0079060). SMP is also grateful to the Defense Acquisition Program Administration and the Agency for Defense Development.

References

1. Chandler, D. W.; Houston, P. L. *J. Chem. Phys.* **1987**, *87*, 1445.
2. Eppink, A. T. J. B.; Parker, D. H. *Rev. Sci. Instrum.* **1997**, *68*, 3477.
3. Gebhardt, C. R.; Rakitzis,T. P.; Samartzis, P. C.; Ladopoulos, V.; Kitsopoulos, T. N. *Rev. Sci. Instrum.* **2001**, *72*, 3848.
4. Lin, J. J.; Zhou, J.; Shiu, W.; Liu, K. *Rev. Sci. Instrum.* **2003**, *74*, 2495.
5. Felder, P.; Haas, B. M.; Huber, J. R. *Chem. Phys. Lett.* **1991**, *186*, 177.
6. Hanisco, T. F.; Kummel, A. C. *J. Phys. Chem.* **1993**, *97*, 7242.
7. Suzuki, T.; Katayanagi, H.; Mo, Y.; Tonokura, K. *Chem. Phys. Lett.* **1996**, *256*, 90.
8. Neyer, D. W.; Heck, A. J. R.; Chandler, D. W. *J. Chem. Phys.* **1999**, *110*, 3411.
9. Brouard, M.; Clark, A. P.; Vallance, C.; Vasyutinskii, O. S. *J. Chem. Phys.* **2003**, *119*, 771.
10. Nishide, T.; Suzuki, T. *J. Phys. Chem. A* **2004**, *108*, 7863.
11. Smolin, A. G.; Vasyutinskii, O. S.; Wouters, E. R.; Suits, A. G. *J. Chem. Phys.* **2004**, *121*, 6759.
12. Kawamata, H.; Kohguchi, H.; Nishide, T.; Suzuki, T. *J. Chem. Phys.* **2006**, *125*, 133312.
13. Zhang, X.-p.; Lee, W.-B.; Zhao, D.-f.; Hsiao, M.-K.; Chen, Y.- L.; Lin, K.-C. *J. Chem. Phys.* **2009**, *130*, 214305.
14. Gough, T. E.; Miller, R. E.; Scoles, G. *J. Chem. Phys.* **1978**, *69*, 1588.
15. Miller, R. E.; Watts, R. O.; Ding, A. *Chem. Phys.* **1984**, *83*, 155.
16. Miller, R. E.; Watts, R. O. *Chem. Phys. Lett.* **1984**, *105*, 409.
17. Ohshima, Y.; Matsumoto, Y.; Takami, M.; Kuchitsu, K. *Chem. Phys. Lett.* **1988**, *152*, 294.
18. Huang, Z. S.; Miller, R. E. *J. Chem. Phys.* **1988**, *89*, 5408.
19. Kudoh, S.; Onoda, K.; Takayanagi, M.; Nakata, M. *J. Mol. Struct.* **2000**, *524*, 61.
20. Li, W.; Chambreau, S. D.; Lahankar, S. A.; Suits, A. G. *Rev. Sci. Instrum.* **2005**, *76*, 063106.
21. Parker, D. H.; Eppink, A. T. J. B. *J. Chem. Phys.* **1997**, *107*, 2357.